Zheng W *et al.* (2021)
Notulae Botanicae Horti Agrobotanici Cluj-Napoca
Volume 49, Issue 1, Article number 12191
DOI:10.15835/nbha49112191
Research Article

Transcriptome-wide identification and characterization of *WD40* genes, as well as their tissue-specific expression profiles and responses to heat stress in *Dimocarpus longan* Lour.

Wei ZHENG[1], Ziwei ZHANG[1], Xuefei YU[2], Tongtong XIE[1], Ning CHEN[1], Wenlan LI[1]*

[1]*Harbin University of Commerce, School of Pharmacy, No. 138, Tongda Street, Daoli District, 150076, Harbin, China; wei2013zheng@163.com; zzw19951216@163.com; xtt15663674920@163.com; chenning1981@126.com; 1296893651@qq.com (*corresponding author)*
[2]*Harbin University of Commerce, School of Library, No. 1, Xuehai Street, Songbei District, 150028, Harbin, China; yuxuefei83@163.com*

Abstract

The WD40 transcription factor (TF) family is widespread in plants and plays important roles in plant growth and development, transcriptional regulation, and tolerance to abiotic stresses. WD40 TFs have been identified and characterized in a diverse series of plant species. However, little information is available on *WD40* genes from *D. longan*. In this study, a total of 45 *DlWD40* genes were identified from *D. longan* RNA-Seq data, and further analysed by bioinformatics tools. Also, the expression patterns of *DlWD40* genes in roots and leaves, as well as responses to heat stress, were evaluated using quantitative real-time PCR (qRT-PCR). We found that the 45 DlWD40 proteins, together with 80 WD40 proteins from *Arabidopsis* and *Zea mays*, could be categorized into six groups. Of these, the DlWD40-4 protein was highly homologous to *Arabidopsis* WDR5a, a protein participating in tolerance to abiotic stresses. Moreover, a total of 25 *cis*-acting elements, such as abiotic stress and flavonoid biosynthesis elements, were found in the promoters of *DlWD40* genes. The *DlWD40-33* gene is targeted by miR3627, which has been proposed to be involved in flavonoid biosynthesis. Using qRT-PCR, ten of the 45 *DlWD40* genes were demonstrated to have diverse expression patterns between roots and leaves, and these ten *DlWD40* genes could also respond to varying durations of a 38 °C heat stress in roots and leaves. The results reported here will provide a basis for the further functional verification of *DlWD40* genes in *D. longan*.

Keywords: bioinformatics analysis; *Dimocarpus longan* Lour; gene expression; *WD40* gene; thermal response

Introduction

Dimocarpus longan Lour. (*D. longan*), a member of the Sapindaceae family, is a perennial evergreen plant that is widely planted in humid and warm subtropical circumstances (Wang *et al.*, 2015). *D. longan* is one of the major commercial crops in South China, Thailand, Vietnam, and other Southeast Asian countries,

Received: 14 Dec 2020. Received in revised form: 06 Feb 2021. Accepted: 17 Feb 2021. Published online: 25 Feb 2021.
From **Volume 49, Issue 1, 2021,** Notulae Botanicae Horti Agrobotanici Cluj-Napoca journal will use article numbers in place of the traditional method of continuous pagination through the volume. The journal will continue to appear quarterly, as before, with four annual numbers.

where the growth environments of *D. longan* are very friendly (Hu *et al.*, 2018b). The pulps, leaves, flowers, and roots of *D. longan* contain a variety of bioactive ingredients, such as flavonoids, tannins, and polysaccharides, thereby serving as traditional Chinese medicine to treat wounds, acariasis, and influenza (Ho *et al.*, 2007; Xue *et al.*, 2015). However, compared with the wide consumption of *D. longan* juicy fruit, the applications of *D. longan* roots and leaves as Chinese medicines have been constrained due to the little accumulation of active secondary metabolites. Moreover, the adverse environmental condition is another important factor negatively affecting the growth and quality of *D. longan*. Our previous studies suggested that the 4 *bZIP* genes that were differently expressed between *D. longan* roots and leaves might be involved in the secondary metabolite accumulations (Zheng *et al.*, 2020). In *D. longan*, the up-regulated expressions of WRKY1, WRKY8, and WRKY50 correspondingly contributed to the tolerance to drought, heat, and cold stresses, respectively (Jue *et al.*, 2018). Therefore, it is urgent to investigate the key TF which not only participate in flavonoid biosynthesis but also enhance abiotic resistances.

WD40, a member of the broadly spread TF family in eukaryote species, is composed of WD40 repeats, which are characterized by a sequence of 40–60 amino acids (van Nocker and Ludwig 2003; Hu *et al.*, 2018a). Each WD40 repeat typically starts with a Glycine-Histidine (GH) pair at the N-terminus and ends with a tryptophan-aspartic acid (WD) pair at the C-terminus (van Nocker and Ludwig 2003; Higa and Zhang 2007). Each WD40 repeat is composed of four-stranded antiparallel ß-sheets, and can interact with other WD40 repeats to fold into a β -propeller, an important structure that enables WD40 to perform many functions, such as mediating the protein-protein interactions (Nash *et al.*, 2001; Fonseca and Rubio 2019; Ma *et al.*, 2019). In addition, WD40 proteins are also involved in a variety of biological processes and tolerance to abiotic stresses (Li *et al.*, 2014; Hu *et al.*, 2018a). WD40 proteins can regulate flavonoid accumulation in various tissues by mediating the expression of flavonoid biosynthesis genes, including *CHS*, *CHI*, *F3H*, and *DFR* (Wu *et al.*, 2015). For example, MdTTG1, a member of the WD40 family from apple, can interact with both bHLH and MYB to initiate the expression of *DFR*, a gene whose high expression promotes the biosynthesis of anthocyanin (An *et al.*, 2012). The PhAN11 protein, the first identified WD40 family protein from *Petunia hybrida* Vilm, was demonstrated to increase the anthocyanin accumulation via activating the expression of the *DFR* gene (de Vetten *et al.*, 1997). *Arabidopsis* TTG1 (homologs to PhAN11) could form four distinct protein complexes (TT2-TT8-TTG1, MYB5-TT8-TTG1, TT2-GL3-TTG1, and TT2-EGL3-TTG1) with MYB or bHLH proteins; these four complexes could up-regulate the expression of the *DFR* gene to increase anthocyanin accumulation (Xu *et al.*, 2014).

In addition to their involvement in the biosynthesis of secondary metabolites, WD40 proteins have also been shown to participate in the tolerance to abiotic stresses, such as salt stress, drought stress, and heat stress. For example, the *TTG1* gene from the *Recretohalophyte limonium* bicolor could help transgenic *Arabidopsis* to resist salt tolerance through both reducing epidermal ion accumulation and increasing osmotic pressure (Yuan *et al.*, 2019). The TaWD40 transcription factor identified from wheat could respond to abiotic stresses. Heterologous over-expression of the *Ta WD40* significantly enhanced the tolerance to salt stress and osmotic stress in *Arabidopsis* (Kong *et al.*, 2015). The tolerance to drought stress was strengthened in *Medicago sativa* L. by enhancing the expression of WD40-1, the mechanism of which was due to the increasing content of anthocyanin (Feyissa *et al.*, 2019). The TAWD protein, a member of the WD40 TF family from *Arabidopsis*, was involved in improving *Arabidopsis* resistance to high-temperature stress through activating the expression of heat-shock response (HSR) genes (Xia 2019).

Although the *WD40* TF gene family has been intensively investigated in a variety of species, including potato, rice, and *Arabidopsis* (van Nocker and Ludwig 2003; Ouyang *et al.*, 2012; Tao *et al.*, 2019), little is known about *WD40* TF genes for *D. longan*. In this study, we identified 45 *DlWD40* genes from *D. longan* RNA-Seq data and used bioinformatics tools to analyse their physiochemical properties, conserved motifs, evolutionary relationships, GO annotations, gene structures, promoter function prediction, protein-protein interactions, and miRNA targets. Additionally, qRT-PCR was used to detect their expression patterns in roots and leaves, as well as in response to heat stress, in order to identify key *WD40* TF genes that both function in

flavonoid accumulation and in tolerance to heat stress. The results of this study will provide a genetic resource for not only improving *D. longan* tolerance to abiotic stresses but also increasing flavonoid accumulation in *D. longan* leaves and roots through genetic engineering.

Materials and Methods

Materials and growth conditions

D. longan plants were planted in a greenhouse maintained at 25 °C and relative humidity of 50%. After 2 months of growth, leaves (picked from the upper peripheral branches) and roots gathered from ten plants. For the heat stress, the 2-month-old *D. longan* plants were exposed to a 38 °C heat stress for 1, 4, 8, or 24 h. Then, the roots and leaves from *D. longan* were collected after heat stress at the given time points. All samples were immediately immersed in liquid nitrogen and then stored in a −80 °C freezer for quantitative real-time PCR (qRT-PCR) analysis.

Identification and bioinformatics analysis of DlWD40 proteins

Based on RNA-Seq data of *D. longan* (NCBI accession number: SRP155595), a total of 45 putative *DlWD40* genes were identified. Using the NCBI CD-Search and the SMART tools, the WD40 domain and the quantities of WD40 repeat for 45 DlWD40 proteins were identified. The molecular weights, protein sequence lengths, aliphatic indices, instability indices, grand average of hydropathicity scores, isoelectric points, subcellular protein localization, motif predictions, miRNA targets, and functional regulatory networks of the *D. longan* DlWD40 proteins were comprehensively investigated using bioinformatics software (Table 1). The *D. longan* miRNAs used for the analysis of miRNA targets were downloaded from the results of Lin *et al.* (2013). Genes from the *D. longan* genome that were highly homologous to the 45 *DlWD40* genes identified from RNA-Seq data were used as representatives to study the *DlWD40* gene structures and *cis*-acting elements. The visualization analysis of gene structures and conserved motifs were achieved using TBtools (Chen *et al.*, 2020). Forty-five DlWD40 proteins, together with 80 WD40 proteins from *Arabidopsis thaliana* and *Zea mays*, were used to construct a phylogenetic tree in MEGA 7.0 using the neighbour-joining method with 1000 bootstrap iterations. The functional classification of DlWD40 proteins into biological process, molecular function, and cellular component were generated by Blast2GO v5.0.

Table 1. On-line software for bioinformatics analysis

Name	Web address	Function
ORFfinder	https://www.ncbi.nlm.nih.gov/orffinder	Open reading frame prediction
NCBI CD search	https://www.ncbi.nlm.nih.gov/Structure/bwrpsb/bwrpsb.cgi/	Conservative domain prediction
SMART	http://smart.embl-heidelberg.de/	Conservative domain prediction
ExPASY	https://web.expasy.org/protparam/	Physical and chemical properties prediction
SOPMA	https://npsa-prabi.ibcp.fr/cgi-bin/npsa_automat.pl?page=npsa_sopma.html	Secondary structure prediction
WoLF PSORT	https://wolfpsort.hgc.jp/	Subcellular localization prediction
MEME	http://meme-suite.org/tools/meme	Conserved motifs prediction
PlantCARE	http://bioinformatics.psb.ugent.be/webtools/plantcare/html/	*Cis* response element prediction
psRNATarget	http://plantgrn.noble.org/psRNATarget/	Plant small RNA target analysis server
STRING	https://string-db.org/cgi/input.pl	Protein-protein interactions prediction

RNA isolation and quantitative real-time PCR analysis

RNA was extracted from the root and leaf tissues of *D. longan* using the cetyltrimethylammonium bromide (CTAB) method (Jaakola *et al.*, 2001). TransScript® One-Step gDNA Removal and cDNA Synthesis SuperMix kits (TransGen Biotech, Beijing, China) were used to obtain the first-strand cDNAs following the manufacturer's instructions. Quantitative real-time PCR (qRT-PCR) reactions were performed to evaluate

the expression levels of *DlWD40* genes using the TransStart® Top Green qPCR SuperMix (TransGen Biotech, Beijing, China) according to the manufacturer's instructions. The reaction system includes 10 μL of 2× TransStart® Top Green qPCR SuperMix, l μL of cDNA template, 7 μL of ddH2O, 1 μL of forwarding primer, and 1 μL of reverse primer (Table 2). The *D. longan tubulin* gene was chosen as a reference gene. The qRT-PCR reaction parameters were set as follows: 95 °C for 1 min, followed by 95 °C for 5 s, 60 °C for 30 s, and 72 °C for 30 s. All assays were performed in triplicate. The $2^{-\Delta\Delta CT}$ method was used to calculate the relative gene expression (Schmittgen and Livak 2008).

Table 2. Primer sequences for qRT-PCR

Gene	Primer sequence
DlWD40-4	F: CAATGGTGCGACAGATGA R: CCTCGGCAATGATAAGACT
DlWD40-13	F: GTAGTGGCTCTGCTGATAA R: CAGTTATGACTCCAACCTTAC
DlWD40-20	F: CAATCCAAGCACATTCAGAG R: CGGTAAGGTTACGACTAGC
DlWD40-21	F: CGGCTGGTAGATTGGAAG R: TGCTGATGGACTGAAGGA
DlWD40-22	F: AGTTGTTGACGACGGAAG R: CAAGCAATGGAGGAAGAGA
DlWD40-25	F: TGTTGAGGAGGTGGTGATA R: GTAAGCAGAAGCCGACAA
DlWD40-31	F: GCCATCAATACAAGCACAA R: AACGAGGTAATCAGACGAAT
DlWD40-32	F: TGCTTCAATGGAGAACGAT R: CAAGGATACTGGTGGAGATT
DlWD40-36	F: TGTGATGCCTCCTTGTCT R: GCTTGTTGATATGCTTCCTAC
DlWD40-38	F: TCCGTCCGAATCCTCATA R: CTGGCATCAACATAAGCATA
Tubulin	F: CTCATGTATGCCAAGCGTGC R: CTCTGCAGACTCAGCACCAA

Results

Identification and structural analysis of DlWD40 TFs from D. longan

Based on Nr annotation, we obtained 45 putative *DlWD40* genes from RNA-Seq data of *D. longan* leaves and roots (accession number: SRP155595). Then CD search and SMART tools were used to further confirm their identities. For convenience, these genes were numbered from *DlWD40-1* to *DlWD40-45* according to the order in which they were identified from RNA-Seq data. In total, 45 DlWD40 proteins could be divided into two groups (Figure 1). The first group, including 34 DlWD40 proteins, was characterized as having only the WD40 domain in each DlWD40. The second group (11 DlWD40 proteins) not only contained the WD40 domain but also possessed other identified domains, such as Cytadhesin-P30, Med15, Bromo-WDR9-I-like, Coatomer-WDAD, Ge1-WD40, DUF4678, NLE, CAF1C-H4-bd, Katanin-con80, ATG16, Ufd2P-core, and ANAPC4.

Figure 1. Identification and structural analysis of DlWD40 proteins
The protein structure is based on the presence of WD40 and other additional domains, as identified by SMART and CD search

Physicochemical properties

The physicochemical properties of DlWD40 proteins, including the length of open reading frames (ORF), molecular weights (MW), isoelectric points (pI), aliphatic indices, instability indices (II), grand average of hydropathicity (GRAVY) scores, and subcellular localizations were evaluated using ExPASY. The results shown in Table 3 indicate that the length of DlWD40 proteins varied from 124 bp to 1286 bp, and the molecular weight ranges from 13,370.22 to 141,013.77 Da. Among 45 DlWD40 proteins, 17 DlWD40s were acidic proteins, and 28 DlWD40s were basic proteins. The subcellular localization analysis showed that nearly half of the DlWD40 proteins were predicted to localize in the nuclear compartment, and the remaining were predicted to localize in the chloroplast, cytoplasm, plasma, mitochondrial, or peroxisome.

Conserved motifs and gene structures

The conserved motifs of 45 DlWD40 proteins were investigated by MEME. To analyse the gene structures, genes from the *D. longan* genome that were highly homologous to 45 *DlWD40* genes from *D. longan* RNA-Seq data were chosen as representatives (Table 4). TBtools was used to display the evolutionary relationship, conserved motifs, and gene structures of the 45 DlWD40 proteins (Figure 2). A total of 15 motifs were identified from DlWD40 proteins. Of these, the motif2 was present in all the 45 DlWD40 proteins. The motif3 and motif4 were also widely spread, conserved by 41 and 43 DlWD40 proteins, respectively. The gene structure analysis showed that the quantities of introns contained by *DlWD40* genes varied significantly. Particularly, there were no introns found in *DlWD40-1*, *DlWD40-10*, *DlWD40-13*, *DlWD40-16*, *DlWD40-20*, *DlWD40-23*, *DlWD40-36*, and *DlWD40-41*. In addition, in group A or group B, formed based on the results of the phylogenetic tree, had similar motif compositions and quantities of introns/exons.

Table 3. Physicochemical properties and subcellular localization of DlWD40 proteins

Name	ID	ORF (aa)	PI	Aliphatic index	MW(Da)	Instability index (II)	GRAVY	Subcellular localization
DlWD40-1	c32248.graph_c0	441	8.82	73.61	48131.50	41.26	-0.349	nuclear
DlWD40-2	c38259.graph_c0	342	8.66	67.54	37961.53	38.53	-5.040	chloroplasmat
DlWD40-3	c33075.graph_c0	332	9.53	78.13	36225.96	33.35	-0.336	nuclear
DlWD40-4	c33149.graph_c0	313	6.78	75.27	34719.94	25.19	-0.322	chloroplasmat
DlWD40-5	c32029.graph_c0	721	8.71	49.24	79614.81	57.48	-0.753	nuclear
DlWD40-6	c29449.graph_c0	1148	5.80	67.78	130309.09	52.31	-0.805	peroxisome
DlWD40-7	c36465.graph_c0	603	5.13	77.15	67847.41	44.98	-0.444	nuclear
DlWD40-8	c11378.graph_c0	540	4.23	74.00	59943.59	38.51	-0.562	cytoplasm
DlWD40-9	c11668.graph_c0	348	4.95	82.93	38507.36	41.32	-0.202	nuclear
DlWD40-10	c29035.graph_c0	380	9.45	85.61	42233.32	38.19	-0.299	chloroplasmat
DlWD40-11	c36606.graph_c0	551	4.77	86.30	60714.61	42.51	-0.337	nuclear
DlWD40-12	c35681.graph_c0	1286	8.71	92.44	141013.77	40.28	-0.107	nuclear
DlWD40-13	c38763.graph_c0	124	6.80	78.55	13370.22	26.39	-0.127	cytoplasm
DlWD40-14	c33142.graph_c0	359	7.64	82.23	39137.13	28.17	-0.251	mitochondrial
DlWD40-15	c35955.graph_c1	176	5.36	75.80	20341.16	61.22	-0.250	chloroplasmat
DlWD40-16	c18112.graph_c0	424	8.10	87.10	47494.79	34.02	-0.303	chloroplasmat
DlWD40-17	c27535.graph_c0	478	8.55	76.30	53388.72	41.47	-5.502	nuclear
DlWD40-18	c31285.graph_c0	357	4.81	67.20	39846.31	38.88	-0.394	nuclear
DlWD40-19	c36726.graph_c0	913	5.30	76.55	99021.77	55.08	-0.452	chloroplasmat
DlWD40-20	c31155.graph_c0	442	8.80	74.77	48653.05	45.08	-0.309	chloroplasmat
DlWD40-21	c26705.graph_c0	497	5.03	73.88	55857.16	40.31	-0.557	nuclear
DlWD40-22	c32711.graph_c0	430	5.74	87.95	47483.61	40.18	-0.205	nuclear
DlWD40-23	c27808.graph_c0	435	8.90	88.48	47548.09	37.14	-0.138	chloroplasmat
DlWD40-24	c32525.graph_c0	425	4.77	77.53	48470.88	47.93	-0.611	nuclear
DlWD40-25	c30425.graph_c0	1188	8.23	73.59	131992.02	40.57	-0.445	plasma
DlWD40-26	c30662.graph_c0	277	6.99	82.27	31226.35	37.79	-0.236	cytoplasm
DlWD40-27	c35209.graph_c0	510	5.97	90.49	5615.29	42.72	-0.299	cytoplasm
DlWD40-28	c33988.graph_c0	226	8.12	87.57	24978.50	28.29	-0.019	mitochondrial
DlWD40-29	c34516.graph_c0	449	5.37	81.32	55698.84	39.88	-0.347	nuclear
DlWD40-30	c31803.graph_c0	511	8.83	76.26	57266.56	43.53	-0.462	nuclear
DlWD40-31	c29207.graph_c0	299	5.78	81.14	33502.76	32.58	-0.205	chloroplasmat
DlWD40-32	c29433.graph_c0	419	4.92	60.79	46840.42	42.15	-0.529	nuclear
DlWD40-33	c29959.graph_c0	371	5.21	87.01	41474.71	29.79	-0.266	mitochondrial
DlWD40-34	c17995.graph_c0	432	5.81	92.92	46319.52	36.14	-0.049	cytoplasm
DlWD40-35	c26597.graph_c0	548	7.65	73.28	58643.42	40.26	-0.341	nuclear
DlWD40-36	c16392.graph_c0	250	9.17	82.56	27531.38	50.07	-0.151	cytoplasm
DlWD40-37	c27876.graph_c0	386	4.97	73.21	42283.02	46.34	-0.291	nuclear
DlWD40-38	c33292.graph_c0	187	5.74	84.01	20548.47	32.28	-0.071	cytoplasm
DlWD40-39	c32008.graph_c0	499	5.62	80.14	55982.30	38.46	-0.248	nuclear
DlWD40-40	c34466.graph_c0	774	5.10	94.43	87650.03	43.41	-0.183	nuclear
DlWD40-41	c31315.graph_c0	630	6.90	67.38	69852.77	40.92	-0.588	nuclear
DlWD40-42	c31433.graph_c0	299	6.41	79.77	33176.17	35.46	-0.338	cytoplasm
DlWD40-43	c35926.graph_c0	348	8.60	62.76	38581.51	40.26	-0.454	nuclear
DlWD40-44	c13993.graph_c0	343	5.61	76.73	37953.84	51.02	-0.225	cytoplasm
DlWD40-45	c31065.graph_c0	350	5.56	69.94	38158.59	39.80	-0.380	nuclear

Table 4. Selected genes from the *D. longan* genome that were highly homologous to *DlWD40* genes identified from the *D. longan* RNA-Seq data

Gene Name	Homologous gene ID	E-value	Identities	Gene name	Homologous gene ID	E-value	Identities
DlWD40-1	Dlo_029802.1	0	99%	*DlWD40-24*	Dlo_007184.1	0	94%
DlWD40-2	Dlo_012102.2	0	94%	*DlWD40-25*	Dlo_011162.1	0	97%
DlWD40-3	Dlo_020391.1	0	100%	*DlWD40-26*	Dlo_009963.1	0	99%
DlWD40-4	Dlo_000498.1	0	99%	*DlWD40-27*	Dlo_017783.1	0	97%
DlWD40-5	Dlo_024415.1	0	100%	*DlWD40-28*	Dlo_023866.1	e^{-160}	100%
DlWD40-6	Dlo_024984.1	0	47%	*DlWD40-29*	Dlo_030348.1	0	83%
DlWD40-7	Dlo_002488.1	0	93%	*DlWD40-30*	Dlo_029559.1	0	98%
DlWD40-8	Dlo_024199.4	0	98%	*DlWD40-31*	Dlo_010650.1	e^{-167}	100%
DlWD40-9	Dlo_015366.1	0	99%	*DlWD40-32*	Dlo_011186.1	0	99%
DlWD40-10	Dlo_023261.1	0	99%	*DlWD40-33*	Dlo_028362.1	0	99%
DlWD40-11	Dlo_030845.1	0	90%	*DlWD40-34*	Dlo_023879.2	0	85%
DlWD40-12	Dlo_000205.1	0	92%	*DlWD40-35*	Dlo_011062.2	0	73%
DlWD40-13	Dlo_028595.1	$5.00E^{-76}$	91%	*DlWD40-36*	Dlo_028595.1	e^{-153}	88%
DlWD40-14	Dlo_014634.5	e^{-162}	78%	*DlWD40-37*	Dlo_014196.1	0	99%
DlWD40-15	Dlo_009332.1	e^{-131}	100%	*DlWD40-38*	Dlo_024747.1	e^{-116}	91%
DlWD40-16	Dlo_012369.1	0	99%	*DlWD40-39*	Dlo_030441.4	0	80%
DlWD40-17	Dlo_019591.1	0	100%	*DlWD40-40*	Dlo_011184.1	0	99%
DlWD40-18	Dlo_009693.1	0	100%	*DlWD40-41*	Dlo_018435.1	e^{-145}	81%
DlWD40-19	Dlo_020796.1	0	89%	*DlWD40-42*	Dlo_007490.2	0	92%
DlWD40-20	Dlo_004272.1	0	100%	*DlWD40-43*	Dlo_006201.1	0	96%
DlWD40-21	Dlo_012604.1	0	94%	*DlWD40-44*	Dlo_007375.1	0	99%
DlWD40-22	Dlo_004320.1	0	95%	*DlWD40-45*	dlo_038010.1	0	97%
DlWD40-23	Dlo_032379.1	0	91%				

Phylogenetic analysis

An unrooted phylogenetic tree was constructed using MEGA 7.0 to analyze the evolutionary relationships among 125 WD40 proteins (45 DlWD40 proteins from *D. longan*, 40 WD40 proteins from *Arabidopsis thaliana*, and 40 WD40 proteins from *Zea mays*) (Figure 3). Apart from six WD40 proteins not classified into any group, a total of 119 WD40 proteins were categorized into six groups following the strategy that was adopted in rice and *Arabidopsis thaliana* (Ouyang *et al.*, 2012). Group 1 was the largest, containing 49 WD40 proteins, whereas group 6 was the smallest, with only 5 WD40 proteins in this group. Importantly, the DlWD40-4 proteins were highly homologous to the *Arabidopsis thaliana* WDR5a protein, a protein involved in tolerance to abiotic stresses (Liu *et al.*, 2018). Although the TTG1 protein from *Arabidopsis thaliana* was another important WD40 protein functioning in anthocyanin accumulation, we, unfortunately, did not find any DlWD40 proteins that were highly homologous to the TTG1 protein.

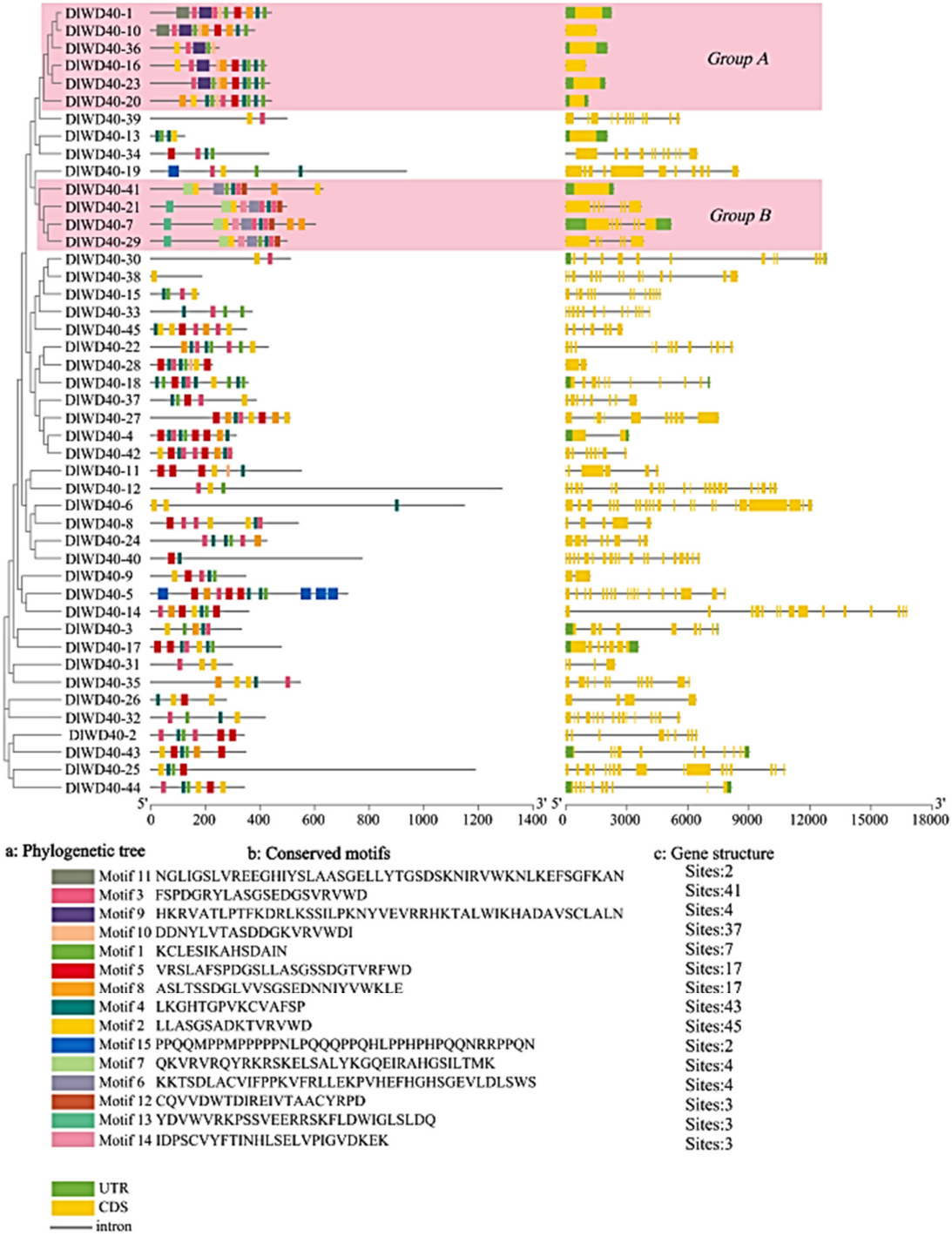

Figure 2. Phylogenetic relationships, cconserved motifs, and gene structure of the *DlWD40* genes
(a) The phylogenetic tree was constructed by Maximum Likelihood (ML) with bootstrap 1000. (b) The conserved motifs was elucidated using MEME. Each motif is represented by a coloured box. (c) Gene structure. The UTR, CDS and introns are represented by green boxes, yellow boxes, and grey lines, respectively. In the legend, capital letters were used to indicate amino acid sequences of 15 motifs and the numbers after sites indicate the number of motifs appearing in DlWD40 proteins

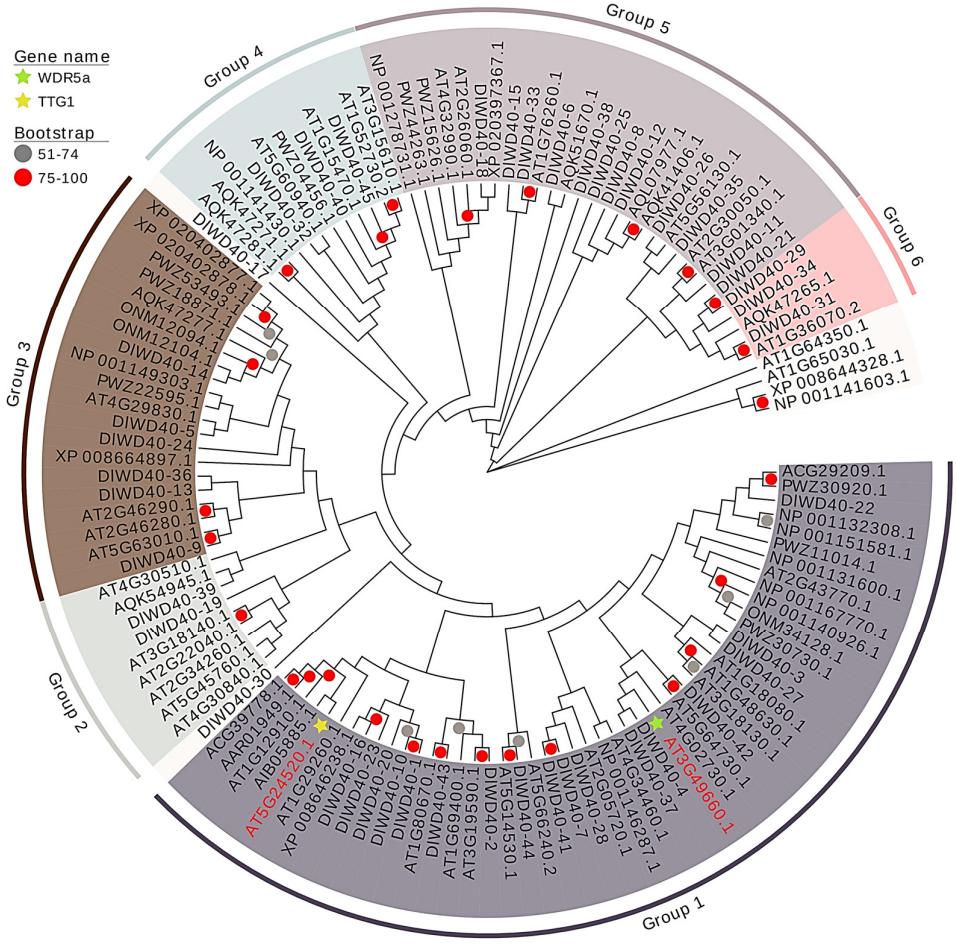

Figure 3. Phylogenetic tree of WD40 proteins from *D. longan*, *Arabidopsis thaliana*, and *Zea mays*

Gene ontology (GO) annotation

The functions of DlWD40 proteins were annotated using Blast2GO v5.2.5. All 45 DlWD40 proteins were classified into three major categories: biological process, cellular component, and molecular function (Figure 4). In the biological process, 45 DlWD40 proteins could be further divided into 13 functional subcategories, of which the cellular process (21 DlWD40 proteins), metabolic process (19 DlWD40 proteins), and cellular component organization or biogenesis (13 DlWD40 proteins) were the first three largest functional subcategories. In molecular function, all 45 DlWD40 proteins were functionally related to binding; thirteen DlWD40 proteins were predicted to be associated with catalytic activity. Three terms were assigned to cellular components, which were intracellular (20 DlWD40 proteins), cellular anatomical entity (21 DlWD40 proteins) and protein-containing complex (16 DlWD40 proteins).

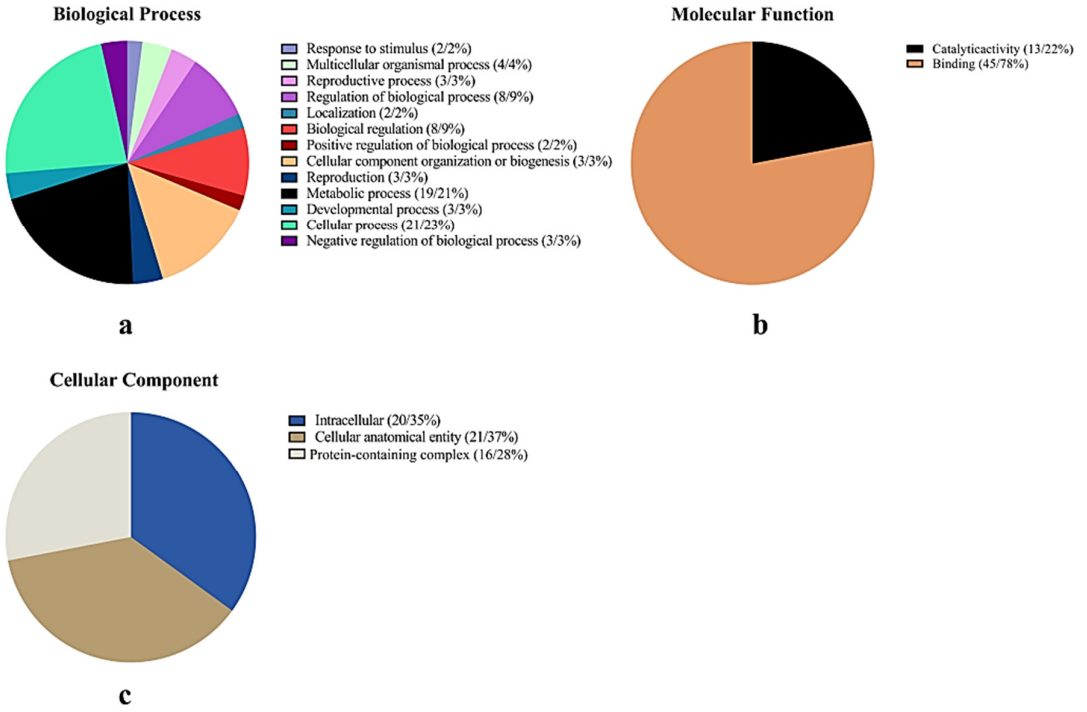

Figure 4. Gene Ontology (GO) annotation results for 45 DlWD40 proteins from *D. longan*. (a) biological processes, (b) molecular functions, and (c) cellular components

Analysis of promoter and miRNA targets

To further predict the putative functions of *DlWD40* genes, PlantCARE was used to analyse the *cis*-acting elements in the promoter region of the 45 *DlWD40* genes. The results are shown in Figure 5: 25 main types of *cis*-regulatory elements were detected, including hormone response elements (abscisic acid, gibberellin, methyl jasmonate, and salicylic acid), abiotic stress response elements (anaerobic, low-temperature, light, drought, and wound), MYB response elements, and other response elements related to plant growth and development. The compositions and quantities of *cis*-elements in the promoter of each *DlWD40* gene are systematically displayed in Figure 5. The light response elements (G-box, I-box, AE-box, and Box-4) that were conserved by all the 45 DlWD40 proteins were found to present in a large number.

miRNAs are a class of single-stranded non-coding RNAs (18–25 nt in length) that negatively regulate gene expression by cleaving targeted mRNAs and repressing translation. In this study, we used psRNATarget to explore the *D. longan* miRNAs that could target on *DlWD40* genes. The results shown in Figure 6 indicate that the regulatory networks of miRNA-gene were complicated. It can be seen that a *DlWD40* gene could be targeted by more than one miRNA, suggesting that the expressions of *DlWD40* genes might be repressed by various miRNAs. It is noteworthy that the expressions of *DlWD40-5*, *DlWD40-6*, and *DlWD40-25* genes were predicted to be negatively regulated by five diverse miRNAs via either cleaving targeted mRNAs or repressing translation. It is noteworthy that miRNA1150, miRNA1078, miRNA2595, miRNA2673a, miRNA2930, and miRNA5170 could regulate different *DlWD40* genes in the same way, while miRNA1150 operated by a different mechanism.

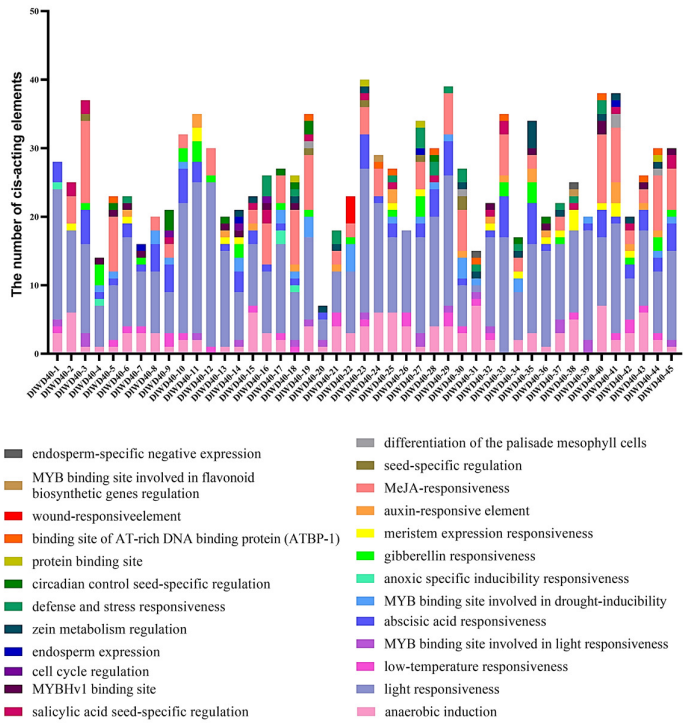

Figure 5. Compositions of the *cis*-acting element of 45 *DlWD40*s from *D. longan*

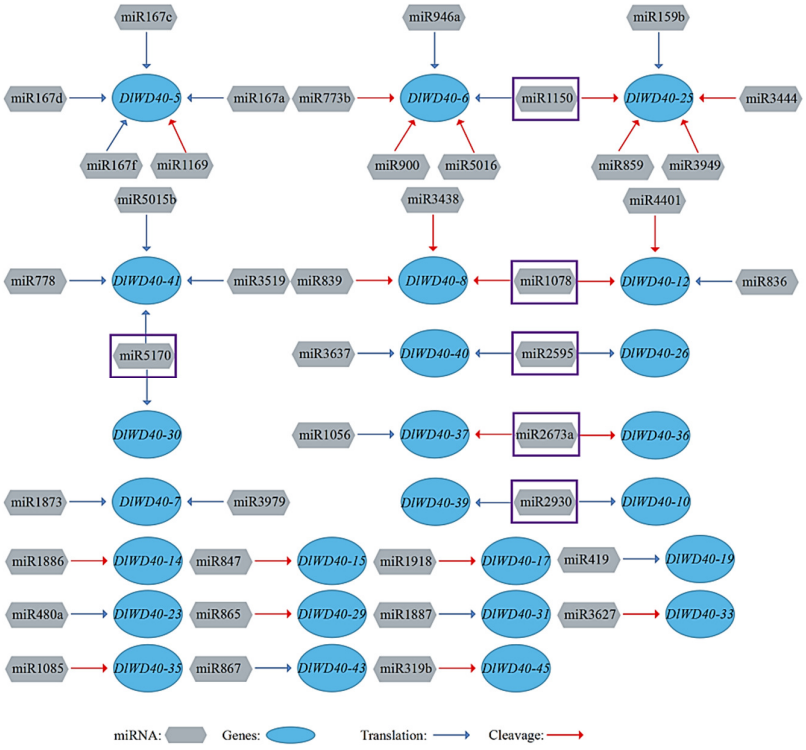

Figure 6. The network of putative miRNA targeting the *DlWD40* genes

The miRNA regulating more than one gene were marked by purple boxes. The top *E*-value was no more than 3.5 (lower *E*-values correspond to higher credibility of miRNA regulatory genes)

Protein-protein interactions

The STRING tool was used in this study to investigate the protein-protein interactions among DlWD40 proteins. STRING was unable to directly study the DlWD40 protein interactions because the *D. longan* genomic data were not available in the STRING database. To solve this problem, the *Arabidopsis* WD40 proteins that were highly homologous to DlWD40 proteins were chosen as representative sequences for the analysis of protein interactions. To a certain extent, the *Arabidopsis* WD40 protein interactions could be used to reveal the interactions of the DlWD40 proteins in *D. longan*, since orthologous proteins usually have similar biological functions (Li *et al.*, 2005).

As shown in Figure 7, 17 DlWD40 proteins (DlWD40-2, DlWD40-4, DlWD40-5, DlWD40-6, DlWD40-8, DlWD40-15, DlWD40-18, DlWD40-20, DlWD40-22, DlWD40-24, DlWD40-28, DlWD40-35, DlWD40-36, DlWD40-40, DlWD40-43, and DlWD40-44) linked with other proteins by purple lines, indicating that the protein-protein interactions were validated experimentally. Among these, DlWD-44 (homologous to AT5G14530), DlWD40-28 (homologous to WDR5b), DlWD40-11 (homologous to AT3G21060), DlWD40-5 (homologous to FY), DlWD40-40 (homologous to APC4), and DlWD40-4 (homologous to WDR5a) could each interact with more than three proteins. Unfortunately, the DlWD39 protein was not found to be homologous to any Arabidopsis WD40 proteins. Also, 13 DlWD40 proteins (DlWD40-1, DlWD40-7, DlWD40-9, DlWD40-10, DlWD40-12, DlWD40-17, DlWD40-21, DlWD40-25, DlWD40-26, DlWD40-29, DlWD40-33, DlWD40-38, and DlWD40-41) were not found to have protein-protein interactions.

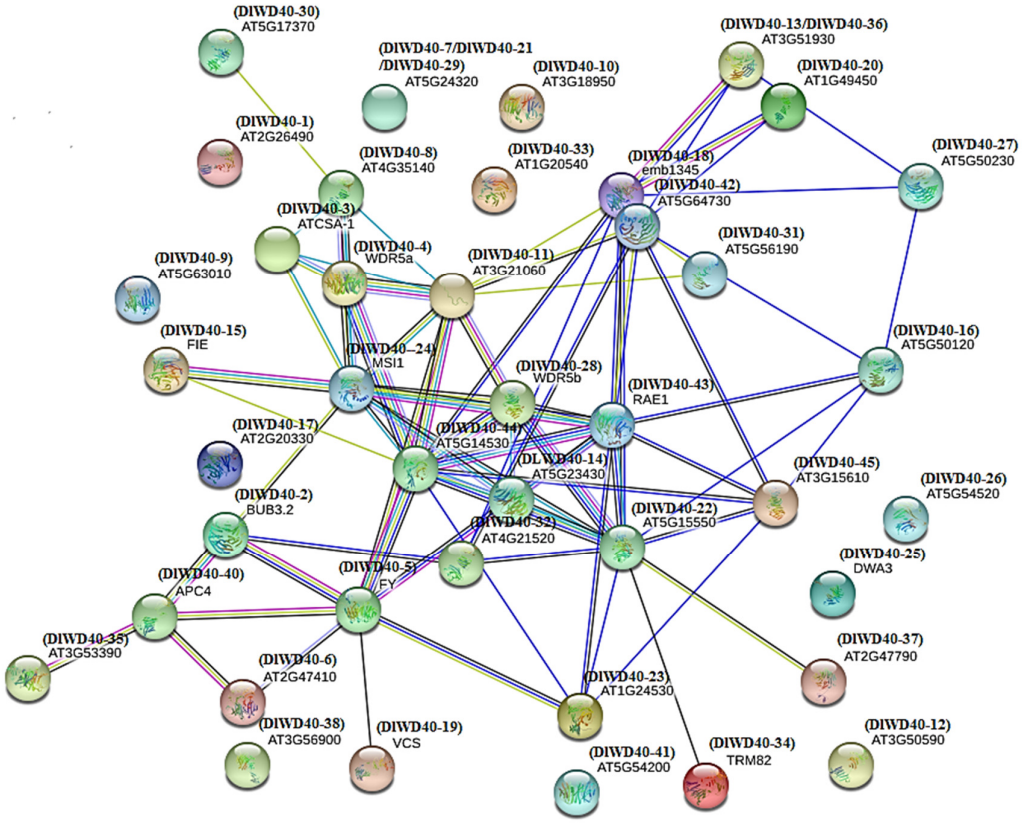

Figure 7. Protein interaction network of DlWD40 proteins from *D. longan*
Purple lines indicate experimentally validated protein interactions; green lines indicate predicted protein interactions based on gene neighbourhood; blue lines indicate predicted protein interactions based on gene co-occurrence; and black lines indicate protein co-expression

Expression levels of DlWD40 genes in root and leaf tissues from D. longan

The expression levels of *DlWD40* genes in *D. longan* roots and leaves were retrieved from *D. longan* RNA-Seq data and shown as a heat map in Figure 8. Ten *DlWD40* genes were identified to exhibit varied expression levels in roots and leaves (*DlWD40-4*, *DlWD40-20*, *DlWD40-21*, *DlWD40-25*, *DlWD40-31*, *DlWD40-13*, *DlWD40-22*, *DlWD40-32*, *DlWD40-36*, and *DlWD40-38*). Next, the expression patterns of these ten *DlWD40* genes were further verified by qRT-PCR, the results of which were generally consistent with that acquired from RNA-Seq data (Figure 9). *DlWD40-13*, *DlWD40-22*, *DlWD40-32*, *DlWD40-36*, and *DlWD40-38* were highly expressed in roots, whereas *DlWD40-4*, *DlWD40-20*, *DlWD40-21*, *DlWD40-25*, and *DlWD40-31* were highly expressed in leaves. It is noteworthy that the expression levels of the *DlWD40-20* between roots and leaves were significantly different. The expression level of the *DlWD40-20* in leaves was nearly 15-fold higher than that in roots.

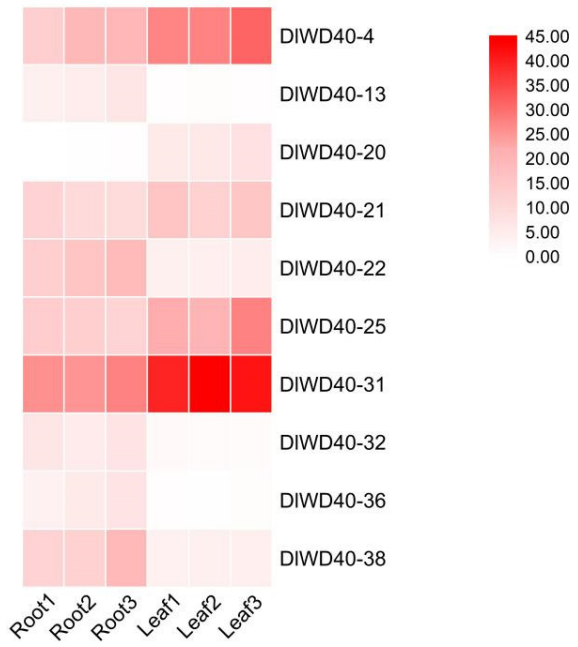

Figure 8. Heatmap showing the expression profiles of the *DlWD40* genes that were differentially expressed between *D. longan* roots and leaves

Expression levels of DlWD40 genes in root and leaf tissues under heat treatments

qRT-PCR was used to further study whether or not these ten tissue-specific expression *DlWD40* genes could respond under 38 °C heat treatments for 1, 4, 8, or 24 h. We found that the expression levels of all ten *DlWD40* genes could be influenced by high-temperature stresses (Figure 10). In general, the expression levels of ten *DlWD40* genes first increased and then decreased during the heat stresses from 0 to 24 h, although some *DlWD40* genes rebounded at 24 h. In roots, the expression levels of the *DlWD40-4*, *DlWD40-20*, *DlWD40-25*, and *DlWD40-31* genes under heat stresses were more than 3-fold higher than the expression levels of 0 h. Of these, the expression level of the *DlWD40-25* gene in leaves was also very high after 24 h heat stress, approximately 3.5-fold that at the 0 h time point.

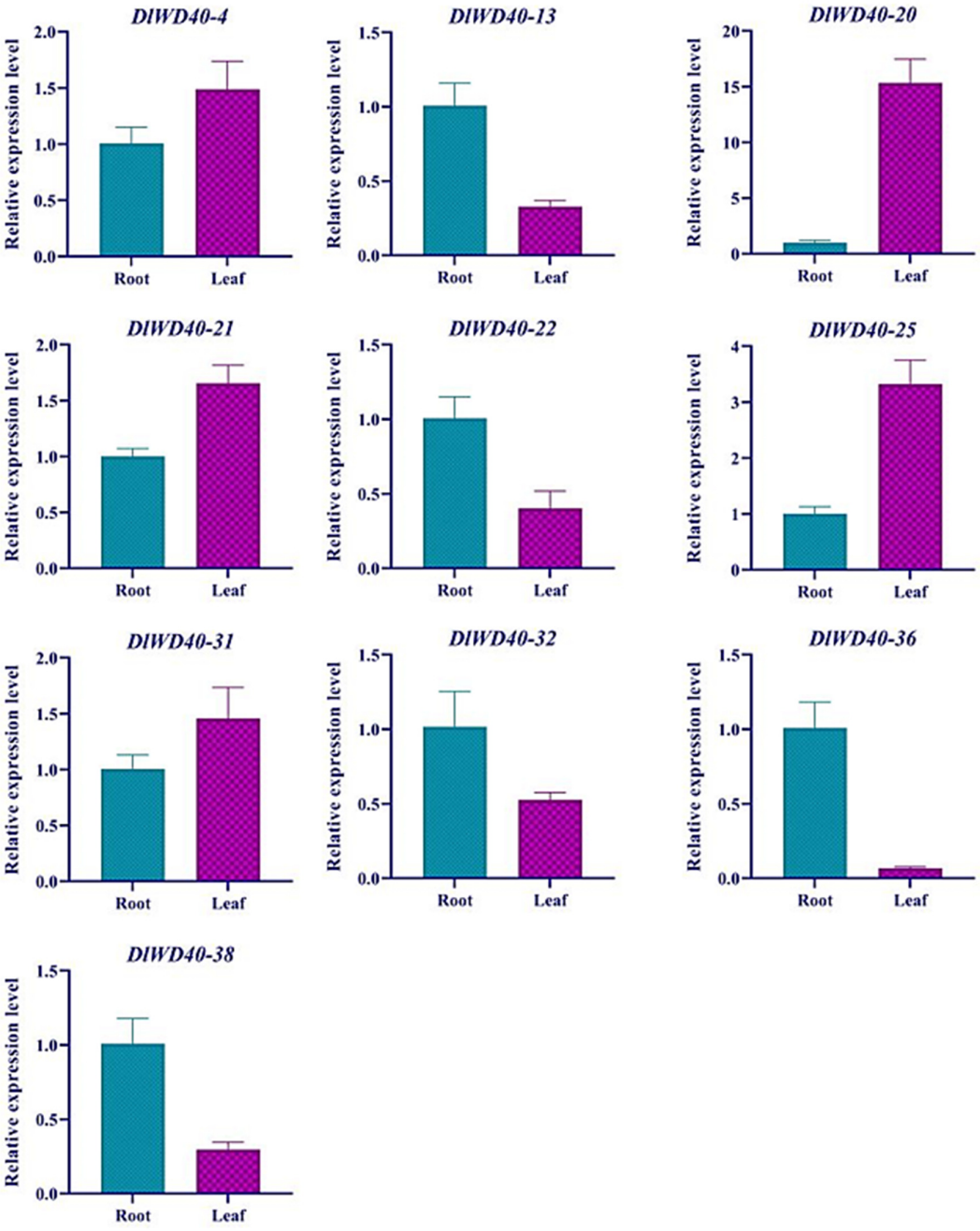

Figure 9. Expression patterns of *DlWD40* genes in roots and leaves of *D. longan*; error bars represent standard error of three independent replicates

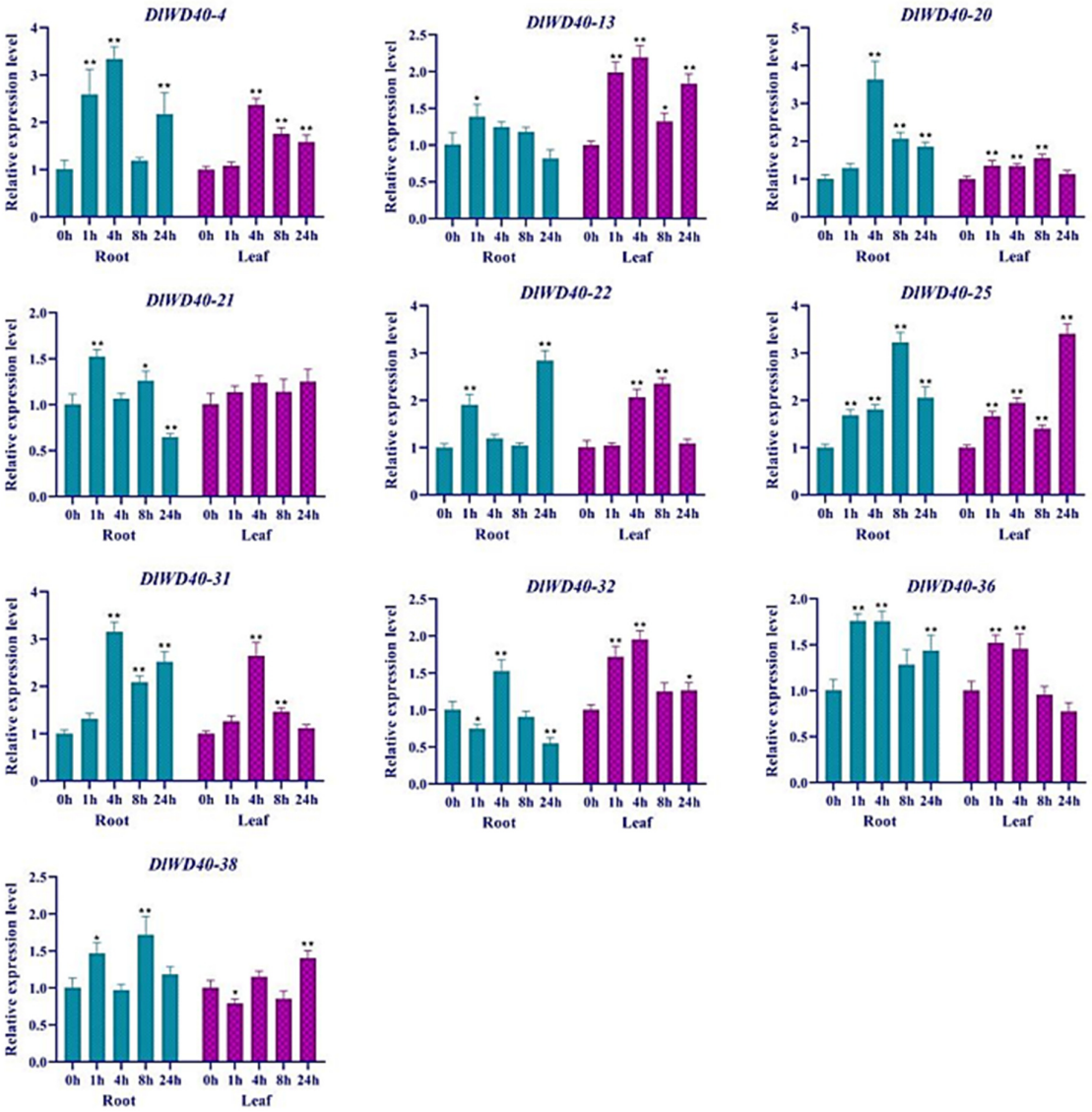

Figure 10. Stress responses of *DlWD40* genes under a 38 °C heat treatment for 1, 4, 8, or 24 h in *D. longan* root and leaf tissues

Asterisks indicate that the value is significantly different from that of the 0 h treatment (* $p < 0.05$, ** $p < 0.01$)

Discussion

D. longan, a sort of very delicious fruit, can serve as traditional Chinese herbal medicine because of the pharmacological activities of its chemical constituents (Xue *et al.*, 2015). *D. Longan* has been extensively used to promote blood metabolism and relieve insomnia (Huang *et al.*, 2019). By contrast, the *D. longan* roots and leaves are also used as traditional Chinese herbal medicine, but are not widely applied due to the little accumulation of flavonoids and other important secondary metabolites. Furthermore, the circumstance (e.g., high temperature) where the *D. longan* usually grows was another important factor adversely affecting their qualities and yields (Jue *et al.*, 2018). Studies have shown that the biosynthesis of flavonoids, a complex biological process, is regulated by the WD40 TF family in plants (Liu *et al.*, 2013). WD40 TFs can interact

with bHLH and MYB TFs to form complexes that could regulate the transcriptional levels of related genes, thereby affecting the anthocyanin synthesis in plants (Qin *et al.*, 2020). In addition, the WD40 TFs have also been shown to be involved in tolerance to abiotic stresses, such as heat, cold, and salt. For example, under the condition of dehydration, the expression level of *Sm WD40-170* gene decreased to enhance the drought tolerance of *Salvia miltiorrhiza* by promoting stomatal closure (Liu *et al.*, 2020). Thus, studying the multifunctional *DlWD40* TF family from *D. longan* might be of great importance for both increasing the flavonoid accumulation and enhancing their tolerance to abiotic stresses.

In this study, a total of 45 *DlWD40* genes were found from RNA-Seq data based on Nr annotation, and their identities were further confirmed using SMART and NCBI CD search tools. An unrooted phylogenetic tree was constructed to analyse the evolutionary relationships of DlWD40 proteins from *D. longan*. Based on the classification strategy followed in the rice and *Arabidopsis* (Ouyang *et al.*, 2012), 45 DlWD40 proteins, together with WD40 proteins from *Arabidopsis thaliana* (monocot) and *Zea mays* (dicot), were divided into six groups. Among these, two WD40 proteins from *Arabidopsis*, TTG1 and WDR5a, attracted our attention due to their involvement in flavonoid biosynthesis. The *Arabidopsis* TTG1 can promote anthocyanin synthesis by positively regulating the expression of *DFR* and other genes. Petunia AN11 and *Fragaria ananassa* TTG1, homologous to *Arabidopsis* TTG1, have also been reported to be involved in the biosynthesis of anthocyanin (Xu *et al.*, 2014). Petunia AN11 can increase anthocyanin accumulation by enhancing the expression of the *DFR* gene (de Vetten *et al.*, 1997). By contrast, the way in which *F. ananassa* TTG1 increases anthocyanin accumulation is different. *F. ananassa* TTG1 increases anthocyanin accumulation by regulating the *BAN* gene (Schaart *et al.*, 2013). However, none of the *DlWD40* genes identified from the *D. longan* RNA-Seq data were homologous to the *Arabidopsis* TTG1. Fortunately, we found a gene (accession NO. Dlo_032775.1) highly homologous to *Arabidopsis* TTG1 in the *D. longan* genome. The reasons why the homologous gene was found in the *D. longan* genome rather than transcriptome is likely because it is expressed neither in roots nor in leaves under normal growth environment. However, we could not exclude that its expression might be induced by other factors. For example, the expression of the *Arabidopsis* TTG1 gene could be induced by abscisic acid (ABA), thereby increasing anthocyanin accumulation (Chen *et al.*, 2020). The *Arabidopsis WDR5a* gene has been shown to be involved in tolerance to drought stress. Under drought stress, the *WDR5a* gene is over-expressed, promoting the accumulation of nitric oxide in roots (Liu *et al.*, 2018). Studies have indicated that the massive accumulation of flavonoids in maize and *Arabidopsis* was a consequence of the increased nitric oxide (Mongin *et al.*, 2012; Tossi *et al.*, 2011). According to the results shown in the phylogenetic tree, the *DlWD40-4* gene was highly homologous to the *Arabidopsis WDR5a* gene. Consequently, it is inferred that the *DlWD40-4* gene might function as a *WDR5a* gene, participating in tolerance to drought stress and flavonoid accumulation.

Diverse *cis*-elements were found in the promoter regions of 45 *DlWD40* genes using PlantCARE. Some of the *cis*-elements were associated with stress responses, suggesting that the DlWD40 TF family from *D. longan* might be involved in tolerance to inhospitable growth conditions. Also, the MeJA-responsiveness element was found in many of the *DlWD40* genes, and its functions have been explored in diverse plant species. For example, MeJA could increase anthocyanin accumulation in apple through enhancing the expression levels of related genes; all these related genes were proved to contain MeJA response elements (Yan *et al.*, 2020). Therefore, the *DlWD40* genes that contain the MeJA-responsiveness element in promoters could be expected to associate with anthocyanin biosynthesis under MeJA induction. In addition, the *cis*-element of MYB binding site involved in flavonoid was found in the promoters of both *DlWD40-24 and DlWD40-38*, which suggest that the expression of these two genes might be triggered by MYB TFs and then participate in the flavonoid biosynthesis in *D. longan*.

miRNAs were also believed to be pivotal factors influencing plant growth and metabolism through post-transcriptional regulation (Wang *et al.*, 2017). A total of 25 *DlWD40* genes were predicted to be targeted by 41 miRNAs using the psRNATarget. Previous studies have shown that the miR3627 is involved in

anthocyanin biosynthesis in *Vitis vinifera* L. (Sunitha *et al.*, 2019) Accordingly, we speculate that the *DlWD40-33* gene is targeted by miR3627 and might be related to anthocyanin biosynthesis.

The expression patterns of 45 *DlWD40* genes were evaluated by RNA-Seq and qRT-PCR, ten members of which were shown to have different expression levels between root and leaf tissues of *D. longan*. Gene expressions were believed to have close relationships with secondary metabolite accumulations. For example, the high expressions of *AcMYB123* or *AcbHLH42* transcription factor genes in *Actinidia* inner pericarp were proved to contribute to anthocyanin synthesis (Wang *et al.*, 2019). As a result, the *DlWD40-20* gene that was highly expressed in leaves was regarded as a candidate gene for further investigation of its involvement in secondary metabolite biosynthesis. One of our future work will focus on the function of *DlWD40-20* gene participating in the accumulation of secondary metabolites by using transgenic technology. Also, these ten tissue-specific *DlWD40* genes were shown to respond to a 38 °C heat stress, whereas they showed diverse expression levels in both roots and leaves. The *TAWD* gene, a member of the *WD40* gene family from *Arabidopsis*, was found to help resist high temperatures (Hu *et al.*, 2018). Therefore, we speculate that *DlWD40* genes with strong thermal responses, including *DlWD40-4*, *DlWD40-20*, *DlWD40-25*, and *DlWD40-31*, deserve further investigation for their putative functions in resisting heat stress.

Conclusions

In this study, bioinformatics tools were used to analyse 45 *DlWD40* genes identified from *D. longan*, including physical and chemical properties, conserved domains, *cis*-acting elements, protein-protein interactions, evolutionary relationships, GO annotations, and miRNA targets. Moreover, the expression pattern of *DlWD40* genes in roots and leaves, as well as the responses to heat stress (38 °C), were analysed by qRT-PCR. Ten of the 45 *DlWD40* genes (*DlWD40-4*, *DlWD40-20*, *DlWD40-21*, *DlWD40-25*, *DlWD40-31*, *DlWD40-13*, *DlWD40-22*, *DlWD40-32*, *DlWD40-36*, and *DlWD40-38*) were differentially expressed in roots and leaves. Of these, the *DlWD40-20* gene in leaves was nearly 15-fold higher than that in roots. All of these ten *DlWD40* genes could respond to heat stress (38 °C). The *DlWD40-4*, *DlWD40-20*, *DlWD40-25*, and *DlWD40-31* genes responded most strongly to heat stress. The data reported here expand our understanding of WD40 TFs and provide gene resources for increasing the content of flavonoid through genetic engineering. Also, our findings will provide a basis for improving abiotic stress resistance in plants using transgenic technologies.

Authors' Contributions

ZW and ZZW conceived and designed the study, as well as wrote the manuscript. ZZW performed the experiments. YXF reviewed and edited the manuscript. XTT, CN and LWL analyzed the data. All authors read and approved the final manuscript.

Acknowledgements

This study was funded by the Young Scholars with Creative Talents at Harbin University of Commerce (2019CX39), and Doctoral Science Foundation (14LG06).

Conflict of Interests

The authors declare that there are no conflicts of interest related to this article.

References

An XH, Tian Y, Chen KQ, Wang XF, Hao YJ (2012). The apple WD40 protein MdTTG1 interacts with bHLH but not MYB proteins to regulate anthocyanin accumulation. Journal of Plant Physiology 169(7):710-717. *https://doi.org/10.1016/j.jplph.2012.01.015*

Chen C, Chen H, Zhang Y, Thomas HR, Frank MH, He Y, Xia R (2020). TBtools - an integrative toolkit developed for interactive analyses of big biological data. Molecular Plant S1674-2052(20):30187-30188. *https://doi.org/10.1016/j.molp.2020.06.009*

Chen JJ, Mei S, Hu YR (2020). 脱落酸激素诱导拟南芥幼苗中花青素的合成 [Abscisic acid induces anthocyanin synthesis in *Arabidopsis* seedlings]. Guihaia 40(08):1169-1180.

de Vetten N, Quattrocchio F, Mol J, Koes R (1997). The *an11* locus controlling flower pigmentation in petunia encodes a novel WD-repeat protein conserved in yeast, plants, and animals. Genes & Development 11(11):1422-1434. *https://doi.org/10.1101/gad.11.11.1422*

Feyissa BA, Arshad M, Gruber MY, Kohalmi SE, Hannoufa A (2019). The interplay between miR156/SPL13 and DFR/WD40-1 regulate drought tolerance in alfalfa. BMC Plant Biology 19(1):434. *https://doi.org/10.1186/s12870-019-2059-5*

Fonseca S, Rubio V (2019). *Arabidopsis* CRL4 complexes: surveying chromatin states and gene expression. Frontiers in Plant Science *https://doi.org/10.3389/fpls.2019.01095*

Higa LA, Zhang H (2007). Stealing the spotlight: CUL4-DDB1 ubiquitin ligase docks WD40-repeat proteins to destroy. Cell Division 2:5. *https://doi.org/10.1186/1747-1028-2-5*

Ho SC, Hwang LS, Shen YJ, Lin CC (2007). Suppressive effect of a proanthocyanidin-rich extract from longan (*Dimocarpus longan* Lour.) flowers on nitric oxide production in LPS-stimulated macrophage cells. Journal of Agricultural and Food Chemistry 55(26):10664-10670. *https://doi.org/10.1021/jf0721186*

Hu R, Xiao J, Gu T, Yu X, Zhang Y, Chang J, Yang G, He G (2018a). Genome-wide identification and analysis of WD40 proteins in wheat (*Triticum aestivum* L.). BMC Genomics 19(1):803. *https://doi.org/10.1186/s12864-018-5157-0*

Hu Z, Zhao L, Hu Z, Wang K (2018b). Hierarchical structure, gelatinization, and digestion characteristics of starch from longan (*Dimocarpus longan* Lour.) seeds. Molecules 23(12):3262. *https://doi.org/10.3390/molecules23123262*

Huang F, Liu H, Zhang R, Dong L, Liu L, Ma Y, ... Zhang M (2019). Physicochemical properties and prebiotic activities of polysaccharides from longan pulp based on different extraction techniques. Carbohydrate Polymers 206:344-351. *https://doi.org/10.1016/j.carbpol.2018.11.012*

Jaakola L, Pirttilä AM, Halonen M, Hohtola A (2001). Isolation of high-quality RNA from bilberry (*Vaccinium myrtillus* L.) fruit. Molecular Biotechnology 19(2):201-203. *https://doi.org/10.1385/MB:19:2:201*

Jue D, Sang X, Liu L, Shu B, Wang Y, Liu C, Xie J, Shi S (2018). Identification of *WRKY* gene family from *Dimocarpus longan* and its expression analysis during flower induction and abiotic stress responses. International Journal of Molecular Sciences 19(8):2169. *https://doi.org/10.3390/ijms19082169*

Kong D, Li M, Dong Z, Ji H, Li X (2015). Identification of TaWD40D, a wheat WD40 repeat-containing protein that is associated with plant tolerance to abiotic stresses. Plant Cell Reports 34(3):395-410. *https://doi.org/10.1007/s00299-014-1717-1*

Li Q, Zhao P, Li J, Zhang C, Wang L, Ren Z (2014). Genome-wide analysis of the WD-repeat protein family in cucumber and *Arabidopsis*. Molecular Genetics and Genomics 289(1):103-124. *https://doi.org/10.1007/s00438-013-0789-x*

Li WH, Yang J, Gu X (2005). Expression divergence between duplicate genes. Trends in Genetics 21(11):602-607. *https://doi.org/10.1016/j.tig.2005.08.006*

Lin Y, Lai Z (2013). Comparative analysis reveals dynamic changes in miRNAs and their targets and expression during somatic embryogenesis in longan (*Dimocarpus longan* Lour.). PloS One 8(4):e60337. *https://doi.org/10.1371/journal.pone.0060337*

Liu WC, Zheng SQ, Yu ZD, Gao X, Shen R, Lu YT (2018). WD40-REPEAT 5a represses root meristem growth by suppressing auxin synthesis through changes of nitric oxide accumulation in *Arabidopsis*. The Plant Journal 93(5):883-893. *https://doi.org/10.1111/tpj.13816*

Liu XF, Feng C, Zhang MM, Yin XR, Xu CJ, Chen KS (2013). The MrWD40-1 gene of Chinese bayberry (*Myrica rubra*) interacts with MYB and bHLH to enhance anthocyanin accumulation. Plant Molecular Biology Reporter 31(6):1474-1484. *Https://doi.org/10.1007/s11105-013-0621-0*

Liu YC, Ma W, Niu JF, Li B, Zhou W, Liu S, ... Wang ZZ (2020). Systematic analysis of SmWD40s, and responding of SmWD40-170 to drought stress by regulation of ABA- and H_2O_2-induced stomal movement in *Salvia miltiorrhiza bunge*. Plant Physiology and Biochemistry 153:131-140. *https://doi.org/10.1016/j.plaphy.2020.05.017*

Ma J, An K, Zhou JB, Wu NS, Wang Y, Ye ZQ, Wu YD (2019). WDSPdb: an updated resource for WD40 proteins. Bioinformatics 35(22):4824-4826. *https://doi.org/10.1093/bioinformatics/btz460*

Mongin AA, Dohare P, Jourd'heuil D (2012). Selective vulnerability of synaptic signaling and metabolism to nitrosative stress. Antioxidants & Redox Signalling 17(7):992-1012. *https://doi.org/10.1089/ars.2012.4559*

Nash P, Tang X, Orlicky S, Chen Q, Gertler FB, Mendenhall MD, ... Tyers M (2001). Multisite phosphorylation of a CDK inhibitor sets a threshold for the onset of DNA replication. Nature 414(6863):514-521. *https://doi.org/10.1038/35107009*

Ouyang Y, Huang X, Lu Z, Yao J (2012). Genomic survey, expression profile and co-expression network analysis of *OsWD40* family in rice. BMC Genomics 13:100. *https://doi.org/10.1186/1471-2164-13-100*

Qin L, Sun L, Wei L, Yuan J, Kong F, Zhang Y, ... Liu S (2020). Maize SRO1e represses anthocyanin synthesis through regulating the MBW complex in response to abiotic stress. The Plant Journal *https://doi.org/10.1111/tpj.15083*

Schaart JG, Dubos C, Romero De La Fuente I, van Houwelingen AM, de Vos RC, Jonker HH, ... Bovy AG (2013). Identification and characterization of MYB-bHLH-WD40 regulatory complexes controlling proanthocyanidin biosynthesis in strawberry (*Fragaria* × *ananassa*) fruits. New Phytologist 197(2):454-467. *https://doi.org/10.1111/nph.12017*

Schmittgen TD, Livak KJ (2008). Analyzing real-time PCR data by the comparative C(T) method. Nature Protocols 3(6):1101-1108. *https://doi.org/10.1038/nprot.2008.73*

Sunitha S, Loyola R, Alcalde JA, Arce-Johnson P, Matus JT, Rock CD (2019). The role of UV-B light on small RNA activity during grapevine berry development. G3: Genes, Genomes, Genetics 9(3):769-787. *https://doi.org/10.1534/g3.118.200805*

Tao N, Zhu W, Gan M, Chen M, Li T, Tendu A... Yang Q (2019). Genome-wide identification and functional analysis of the WDR protein family in potato. 3 Biotech 9(11):432. *https://doi.org/10.1007/s13205-019-1965-4*

Tossi V, Amenta M, Lamattina L, Cassia R (2011). Nitric oxide enhances plant ultraviolet-B protection up-regulating gene expression of the phenylpropanoid biosynthetic pathway. Plant, Cell & Environment 34(6):909-921. *https://doi.org/10.1111/j.1365-3040.2011.02289.x*

van Nocker S, Ludwig P (2003). The WD-repeat protein superfamily in *Arabidopsis*: conservation and divergence in structure and function. BMC Genomics 4(1):50. *https://doi.org/10.1186/1471-2164-4-50*

Wang B, Tan HW, Fang W, Meinhardt LW, Mischke S, Matsumoto T, Zhang D (2015). Developing single nucleotide polymorphism (SNP) markers from transcriptome sequences for identification of longan (*Dimocarpus longan*) germplasm. Horticulture Research 2:14065. *https://doi.org/10.1038/hortres.2014.65*

Wang L, Tang W, Hu Y, Zhang Y, Sun J, Guo X, ... Liu Y (2019). A MYB/bHLH complex regulates tissue-specific anthocyanin biosynthesis in the inner pericarp of red-centered kiwifruit *Actinidia chinensis* cv. Hongyang. The Plant Journal 99(2):359-378. *https://doi.org/10.1111/tpj.14330*

Wang M, Gao Y, Qu P, Qing S, Qiao F, Zhang Y, Mager J, Wang Y (2017). Sperm-borne miR-449b influences cleavage, epigenetic reprogramming and apoptosis of SCNT embryos in bovine. Scientific Reports 7(1):13403. *https://doi.org/10.1038/s41598-017-13899-8*

Wu H, Lv H, Li L, Liu J, Mu S, Li X, Gao J (2015). Genome-wide analysis of the AP2/ERF Transcription factors family and the expression patterns of *DREB* genes in moso bamboo (*Phyllostachys edulis*). PloS One 10(5):e0126657. *https://doi.org/10.1371/journal.pone.0126657*

Xia KW (2019). 拟南芥WD40家族蛋白TAWD在抵御高温胁迫中的功能研究 [Function study of the WD40-repeat protein TAWD in *Arabidopsis* thermotolerance]. Central China Normal University.

Xu W, Grain D, Bobet S, Le Gourrierec J, Thévenin J, Kelemen Z, Lepiniec L, Dubos C (2014). Complexity and robustness of the flavonoid transcriptional regulatory network revealed by comprehensive analyses of MYB-bHLH-WDR complexes and their targets in *Arabidopsis* seed. New phytologist 202(1):132-144. *https://doi.org/10.1111/nph.12620*

Xue Y, Wang W, Liu Y, Zhan R, Chen Y (2015). Two new flavonols glycosides from *Dimocarpus longan* leaves. Natural Product Research 29(2):163-168. *https://doi.org/10.1080/14786419.2014.971318*

Yan J, He L, Xu S, Wan Y, Wang H, Wang Y, Yu L, Zhu W (2020). Expression analysis, functional marker development and verification of *AgFNSI* in celery. Scientific Reports 10(1):531. *https://doi.org/10.1038/s41598-019-57054-x*

Yuan F, Leng B, Zhang H, Wang X, Han G, Wang B (2019). A WD40-repeat protein from the recretohalophyte *Limonium bicolor* enhances trichome formation and salt tolerance in *Arabidopsis*. Frontiers in Plant Science 10:1456. *https://doi.org/10.3389/fpls.2019.01456*

Zheng W, Xie, TT, Yu XF, Ning C, Zhang ZW (2020). Characterization of *bZIP* transcription factors from *Dimocarpus longan Lour.* and analysis of their tissue-specific expression patterns and response to heat stress. Journal of Genetics 99:69. *https://doi.org/10.1007/s12041-020-01229-3*